0273-2289/96/5758—0581$8.00

Hydrodynamics of Bioreactor Systems for Liquid–Liquid Contacting

C. Tsouris,* H. M. Lizama,
M. A. Spurrier, T. L. Takeuchi, and T. C. Scott

Oak Ridge National Laboratory,
PO Box 2008, Oak Ridge, TN 37831–6226

ABSTRACT

Two liquid–liquid bioreactors, a stirred-tank and a novel electrostatic-dispersion system, are being used to investigate biodesulfurization of oil by sulfate-reducing bacteria (SRB). The hydrodynamic behavior of both bioreactors under various operating conditions is discussed in this article. The total liquid volume of the stirred-tank system is 1 L in a 1.5-L cylindrical tank equipped with two baffles and two Rushton-type six-blade impellers. The steady-state average drop size (d_{32}) was determined by a video technique, and correlated with operating conditions, physical properties, and system geometry. Although the stirred-tank geometry was not standard, the d_{32} correlation was found to be in good agreement with correlations reported in the literature. For the electrostatic dispersion system, a 0.25-L column was used with kerosene as the continuous phase and water containing SRB as the dispersed phase. Microdroplets were obtained by the break-up of the aqueous phase meniscus at the tip of a capillary tube using pulsed direct current (dc) electric fields. The size of the drops ejected from the capillary was measured as a function of the intensity of the applied voltage. Preliminary results showed no deleterious effect of electrospray dispersion on bacteria viability.

Index Entries: Sulfate-reducing bacteria; electorstatic dispersion; electrostatic spraying; liquid contactor.

Nomenclature: a_i, drop diameter (m); d_{32}, Sauter mean diameter defined by Eq. (1) (m); d_i, impeller diameter (m); N, agitation speed (s^{-1}); l, Kolmogorov microscale (m); sulfate-reducing bacteria, SRB; We, Weber number defined by Eq. (3), represents the ratio of destructive over cohesive forces (dimensionless); ε, energy dissipation ($m^2 \cdot s^{-3}$); ν, kinematic viscosity ($m^2 \cdot s^{-1}$); ρ_c, density of the continuous phase ($kg \cdot m^{-3}$); σ, surface tension ($N \cdot m^{-1}$); ϕ, dispersed-phase volume fraction (dimensionless).

INTRODUCTION

In several bioprocessing applications, efficient contact of two liquid phases in a bioreactor is required. One of these phases carries a biocatalyst in the form of enzymes, bacteria, or other entities of biological origin. The other liquid phase

*Author to whom all correspondence and reprint requests should be addressed. E-mail: tsourisc@ornl.gov

carries a reactant component that, in the presence of the biocatalyst, is converted into a product of interest. The biocatalytic activity may occur either in the bulk liquid, where the biocatalyst is suspended, or at the interface between the two phases. In either case, it is desirable to have high interfacial area for mass transport between the two phases, so that mass-transport limitations are eliminated. The interfacial area is enhanced by providing energy into the system, either by mechanical agitation or by electric means. When two liquid phases are contacted in a tank, one of them forms droplets in the other. The initial conditions determine which phase will form drops (dispersed) and which will be the surrounding phase (continuous). The size of the droplets is a function of the system's geometry, the physical properties of both liquids, and the energy provided to the system.

An example of such a liquid–liquid system is biodesulfurization of crude oil. In this case, the biocatalyst is bacteria, e.g., sulfate-reducing bacteria (SRB), immersed in an aqueous phase in contact with the oil phase in a bioreactor. Biodesulfurization of crude oil is an alternative to conventional energy-intensive desulfurization processes, which require high pressure and temperature operations. In any crude oil biodesulfurization scheme, the organosulfur substrate species must be available to the biocatalyst. This is ensured by increasing the interfacial area of contact between the two phases through vigorous agitation of the dispersion or by using other means of creating fine dispersions, such as electrospraying of the aqueous phase containing the biocatalyst in a continuous oil phase.

The objectives of the present study are:

1. To study the hydrodynamic behavior of a stirred-tank bioreactor;
2. Introduce an advanced bioreactor for liquid–liquid contacting;
3. Study the hydrodynamics of the new electrospray bioreactor; and
4. Study viability and growth of bacteria after passing through an electrospray nozzle.

MATERIALS AND METHODS

Stirred-Tank Contactor

The stirred-tank contactor consists of an Omni-culture bench-top fermentor (VirTis Co., Gaedinger, NY) with a vessel capacity of 2 L. Details of the reactor geometry and dimensions are listed in Table 1 and Fig. 1. Experiments were conducted with a kerosene (dispersed)/water (continuous) system. The interfacial tension of this system was measured by a Fisher Autotensiomat Instrument (Fisher Scientific, Pittsburgh, PA) and found to be 28 dyn/cm for 25°C and 26.5 dyn/cm for 40 and 55°C. The reactor was operated anaerobically in batch mode with hydrogen continuously flowing through the free space above the liquid dispersion. The temperature of the reaction mixture was controlled using a heating probe and monitored by a thermocouple. Ports were included in the system for sampling, gas flow, and sparging where necessary. A rubber septum was used for injecting inoculum or reducing agent for the removal of oxygen. Fittings, tubing, and the impeller assembly were all made of stainless steel. The inoculum consisted of 7 mL of a bacterial culture adapted to biphasic growth by being maintained in a 1:1 volume ratio of media and kerosene. Bacterial growth was monitored by direct microscopic count. Experiments were conducted at three temperatures (25, 40, and 55°C), four stirring speeds (300, 350, 400, and 450 rpm), and three phase volume fractions of

Table 1
Stirred-Tank Dimensions

	Symbol	Value
Number of impellers	n_i	2
Number of blades per impellers	n_p	6
Number of baffles	n_b	2
Impeller diameter	d_i	5 cm
Reactor diameter	d_r	10.2 cm
Width of impeller blade	w_i	0.9 cm
Height of impeller blade	h_i	0.9 cm
Width of baffle	w_b	1.6 cm
Reactor height (liquid)	h_R	14 cm
Liquid volume	V_l	1 L

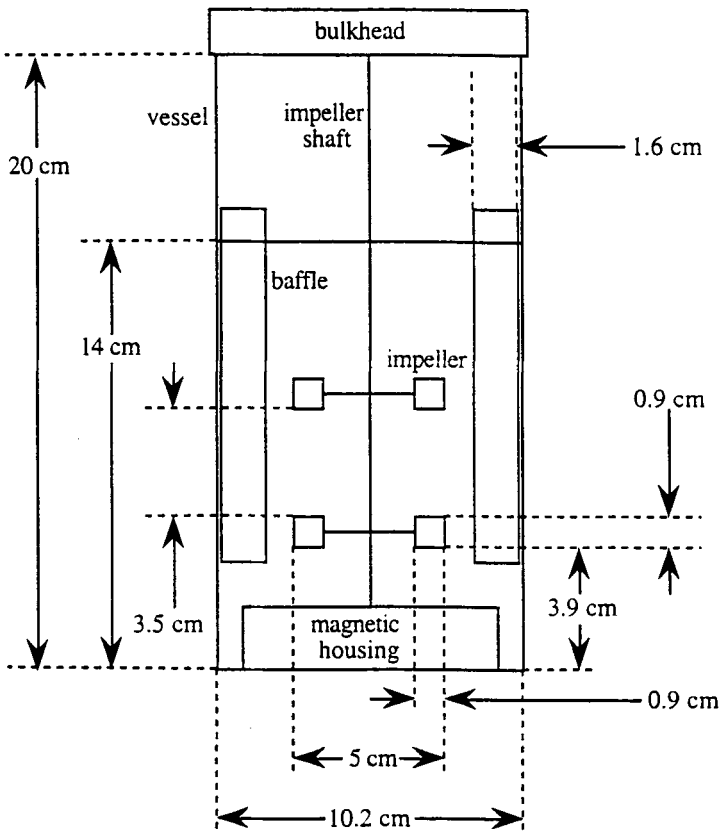

Fig. 1. Geometry of the stirred-tank reactor.

kerosene in water (10, 18, and 25%). In all experiments conducted using the stirred tank, the organic phase (kerosene) was dispersed in the aqueous phase.

Drop Size Measurements

A video technique similar to the one reported by Pacek et al. *(1)* has been developed as shown in Fig. 2. A rigid fiberoptic bundle was bent by 90° at the tip to

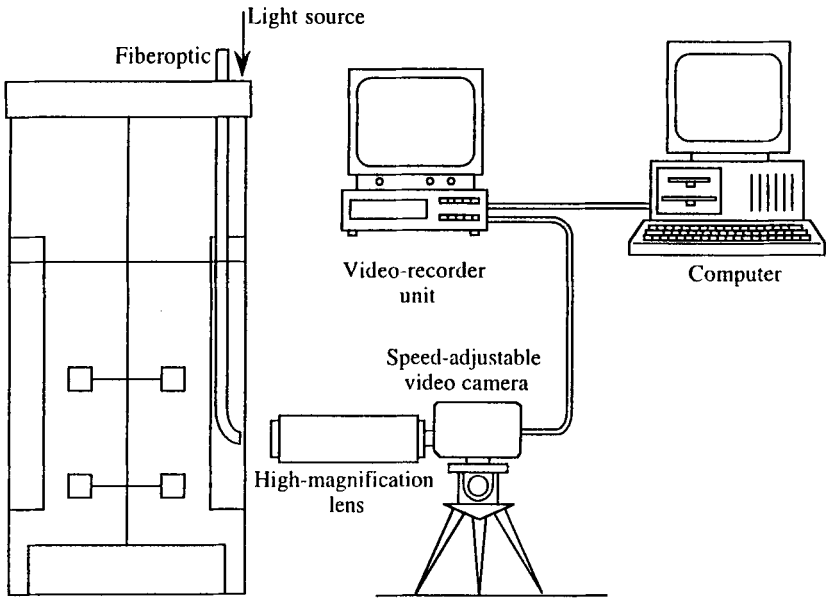

Fig. 2. Apparatus for optical drop size measurements.

illuminate a control volume near the wall where droplets move freely in and out. Although there are strong inhomogeneities in the distribution of the energy dissipation in a stirred tank *(2)*, it has been shown in the literature that the drop size does not vary significantly between the impeller region and the circulation region (near the wall) owing to large convective flow created by Rushton impellers *(3)*. These two regions are associated with extreme values of energy dissipation, the maximum occurring in the impeller region and the minimum in the circulation region. The droplets inside the illuminated control volume are magnified by a high-magnification lens (Questar QM100 from Questar Corp., New Hope, PA) and video-taped by a high-speed video camera (TC651EA from Burle Security Products, Lancaster, PA). The magnification provided by the Questar QM100 is adjustable. Calibration was obtained from pictures of a known-diameter wire taken before each experiment. Drop diameters were measured using Global Lab Image, an image-processing and analysis system for Microsoft Windows (Data Transmission, Malboro, MA), based on frame-by-frame analysis of the video data.

Electrospray

In many liquid–liquid and gas–liquid systems, the dispersed drops or bubbles are in the millimeter size range. In this study, a significant performance was achieved by dispersing one fluid efficiently into another, in the form of micrometer-sized drops or bubbles by using electric fields.

In a review article by Bailey *(4)*, the mechanism of electrostatic spraying is shown to be the result of the interaction between surface charge on a fluid meniscus and an externally applied field. The presence of the electric field drives charge carriers from the bulk of the dispersed liquid to the surface very rapidly. The charge accumulation on the interface causes an outward-pointing force to appear that leads to the break-up of the fluid meniscus into small droplets. Through the

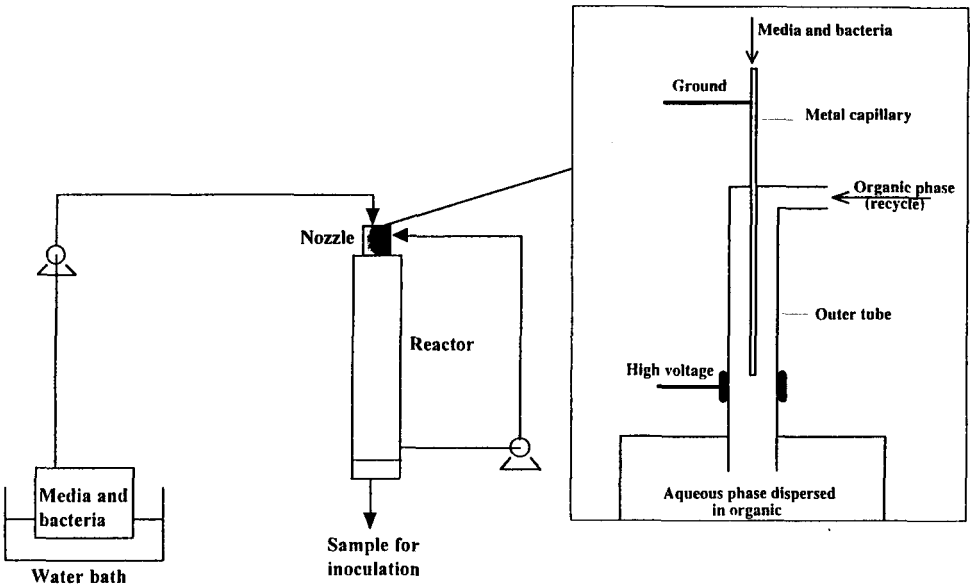

Fig. 3. Flow diagram of the electrospray bioreactor with details of the electrospray nozzle.

years, this technique has found important applications in such areas as painting, printing, and agriculture, as well as liquid extraction (*5*) and materials processing (*6*).

In a recent study, Scott et al. (*7*) successfully employed an electrically driven emulsion-phase contactor for an enzymatic reaction. This work led to the idea of using electrospray systems in microbial reactions. Two examples of such applications in liquid–liquid systems are (1) petroleum biodesulfurization; and (2) biotransformation of coal-derived liquids.

Electrospray Contactor

The electrospray contactor used in this study consists of two parts: (1) the electrospray nozzle and (2) the main reactor (Fig. 3). Details of the electrospray nozzle are shown in Fig. 3. The biocatalyst is suspended in an aqueous medium and is sprayed at the tip of a metal capillary tube because of an electric field between a high-voltage electrode and the grounded capillary tube. The high-voltage electrode is mounted on the outside wall of a dielectric tube, made of Teflon, surrounding the capillary tube. An organic liquid (kerosene) is used between the capillary tube and the dielectric tube in order to avoid accumulation and coalescence of aqueous droplets between the two electrodes. This liquid is used as continuous phase in the bioreactor and is continuously recycled as shown in Fig. 3. A pulsed dc high-voltage signal is applied on the electrode in which both voltage and current are monitored by a digital oscilloscope. The peak of the applied voltage is approx 20 kV, whereas the peak current is approx 0.2 mA. Power consumption, as calculated from voltage and current measurements, was approx 1 W.

The dispersion formed at the nozzle is introduced in the bioreactor, which is a cylindrical vessel of 2.5-cm internal diameter and 30-cm length. The droplets travel through the reactor and coalesce at the liquid–liquid interface located at the bottom of the bioreactor. The aqueous medium with the biocatalyst is then

transferred from the bottom of the bioreactor to the recycle vessel. A small portion of the aqueous droplets is recycled with the kerosene phase through the outer annulus of the nozzle, and it was found that these droplets do not affect the spraying process. The flow rate of the aqueous phase containing the biocatalyst was 1–4 mL/min, whereas the recycling flow rate of kerosene was 50–100 mL/min. This system is, therefore, more suitable for those applications in which a relatively low-volume fraction of an aqueous phase is needed to be dispersed into an organic phase. The drop size obtained at electrospray conditions was measured by a Coulter LS130 instrument.

Biocatalyst

The biocatalyst used in this study is SRB. Growth media consisted of 0.5 g Na_2SO_4, 1.0 g $MgSO_4$, 1.8 g citric acid, 0.4 g $CaCl_2$, 0.5 g NH_4Cl, 0.25 g K_2HPO_4, 2.9 mL sodium lactate syrup, 0.5 g yeast extract, 0.5 g $FeSO_4$, 5.0 mL butyric acid (5.18%), and 0.0485 g cysteine. The media pH was adjusted to 7.0 with 1.0*M* NaOH. An inoculum of 0.7% (v/v) was used.

RESULTS

Stirred-Tank Contactor

The steady-state average drop size was determined in terms of the Sauter mean diameter, d_{32}, by the video technique described in section on Drop Size Measurements. Steady-state conditions were assumed after an equilibration time of 15 min. The Sauter mean diameter is relevant to mass-transport calculations and is defined by:

$$d_{32} = \frac{\sum_{i=1}^{n} a_i^3}{\sum_{i=1}^{n} a_i^2} \qquad (1)$$

where a_i is the drop diameter and n the number of drops counted. Approx 300 drops were counted for each set of conditions. To determine the confidence of droplet diameter measurements, one set of video data was analyzed in triplicate. When the reactor operated at 350 rpm, at a temperature of 40°C, and with a kerosene volume fraction of 18%, d_{32} values obtained were 0.0457, 0.0481, and 0.0490 cm. This corresponds to a mean d_{32} value of 0.0476 cm ± 3.56%.

Drop Size Correlations

The d_{32} data were compared to a number of established correlations for liquid–liquid dispersions that take into account agitation rates, volume fraction, energy dissipation, and physical properties. The objective of these comparisons was to determine quantitatively the effect of the geometrical differences between standard stirred tanks with Rushton turbines as reported by other researchers *(1–3,8–10)*.

Coulaloglou and Tavlarides *(3)* suggested the following correlation for the d_{32}:

$$(d_{32}/d_i) = 0.081\ (1 + 4.47\phi)\ (\mathrm{We})^{-0.6} \qquad (2)$$

$$\mathrm{We} = (N^2\,(d_i)^3 \rho_c/\sigma \qquad (3)$$

where d_i is the impeller diameter, ϕ is the dispersed-phase volume fraction (holdup), We is the Weber number, N is the impeller speed, ρ_c is the continuous

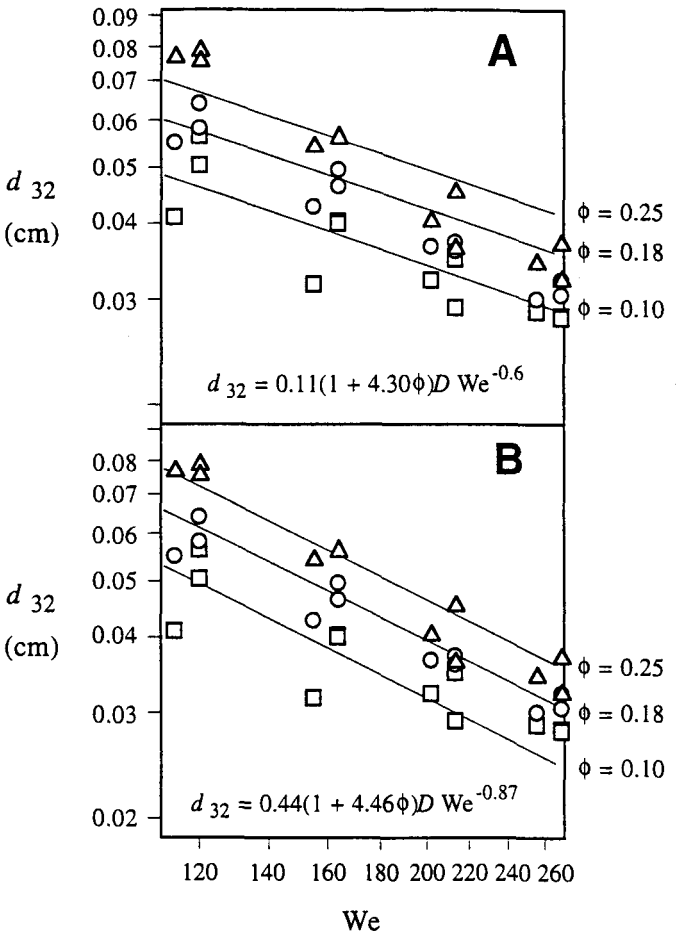

Fig. 4. Correlations of the average drop size with dispersed-phase volume fraction and Weber number; (A) $d_{32} \sim We^{-0.6}$; (B) $d_{32} \sim We^{(parameter)}$.

phase density, and σ is the interfacial surface tension. The constants in Eq. (2) were tested against the d_{32} data for the kerosene/water system obtained in this study using a statistical software package. From a nonlinear fitting program, the optimal relationship was:

$$(d_{32}/d_i) = 0.114\ (1 + 4.30\phi)\ (We)^{-0.6} \quad (4)$$

Figure 4A shows the d_{32} data compared to the correlation of Eq. (4). The –0.6 power in Eq. (4) is theoretically predicted by assuming isotropic turbulence *(10)*. By optimizing the power function, the following relationship is obtained:

$$(d_{32}/d_i) = 0.440\ (1 + 4.56\phi)\ (We)^{-0.87} \quad (5)$$

Figure 4B shows the d_{32} data compared to the correlation of Eq. (5). The correlation values obtained for the various relationships, including a correlation by Calderbank *(9)*, are presented in Table 2. The results suggest that the drop size created by the stirred tank of this study is well predicted by existing correlations, and only a small improvement is achieved by optimizing the constants of these

Table 2
Drop-Size Correlations for Stirred-Tank Contactors

Relationship	Eq. no.	Ref.	r^2
$(d_{32}/d_i) = 0.081\ (1 + 4.47\phi)\ (We)^{-0.6}$	(2)	*(3)*	0.93
$(d_{32}/d_i) = 0.114\ (1 + 4.30\phi)\ (We)^{-0.6}$	(4)	This work	0.94
$(d_{32}/d_i) = 0.440\ (1 + 4.56\phi)\ (We)^{-0.87}$	(5)	This work	0.95
$(d_{32}/d_i) = 0.06\ (1 + 9\phi)\ (We)^{-0.6}$	—	*(9)*	0.90

correlations. This happens even though the geometry of the stirred tank used in this study is significantly different from the standard stirred-tank geometry of one, instead of two, six-blade Rushton turbines and four, instead of two, buffles.

Drop Size Distributions

Measurements of the drop size distribution, plotted in Fig. 5 in the form of cumulative number fraction of drops vs the drop volume, suggest that at a lower agitation speed, the drop size distribution of kerosene dispersed in water is broader and the average drop size is larger.

Effect of Cells and Medium on Drop Size

The effect of addition of nutrients (medium) to the aqueous phase with and without cells is shown in Fig. 6. The addition of medium without cells to the aqueous (continuous) phase had an insignificant effect on the average drop size of kerosene. However, the drop size was increased after addition of cells with medium. This behavior suggests that SRB may not produce any surface active substances, which in general result in lower surface tension and smaller drop size. Furthermore, their presence in the aqueous phase either enhances coalescence, decreases breakage of kerosene drops, or both. This phenomenon needs further investigation because of the importance of drop size on mass-transfer efficiency. An increase in the drop size is expected to decrease the mass-transfer rate.

Cell-Eddy Interactions

The smallest eddy size in an isotropic turbulent flow is the Kolmogorov microscale given by *(10)*:

$$l = 2\ [(\nu^3/\varepsilon)]^{1/4} \tag{6}$$

where ν is the kinematic viscosity and ε is the energy dissipation. Formulas to calculate the energy dissipation are given elsewhere *(10)*. Assuming isotropic turbulence and using the energy dissipation at the tip of the impeller, where it has a maximum value, the scale of the smallest eddy size was calculated as a function of the agitation speed. In these calculations, the presence of the drop phase was not considered. Results showed that, at the highest agitation speed used in this study (450 rpm), the microscale is approx 10 μm, which is one order of magnitude

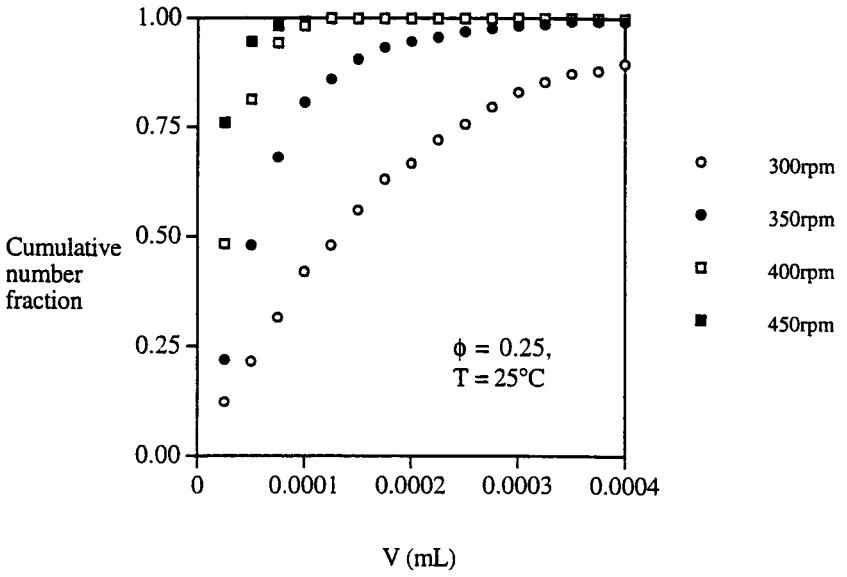

Fig. 5. Drop size distribution measurements.

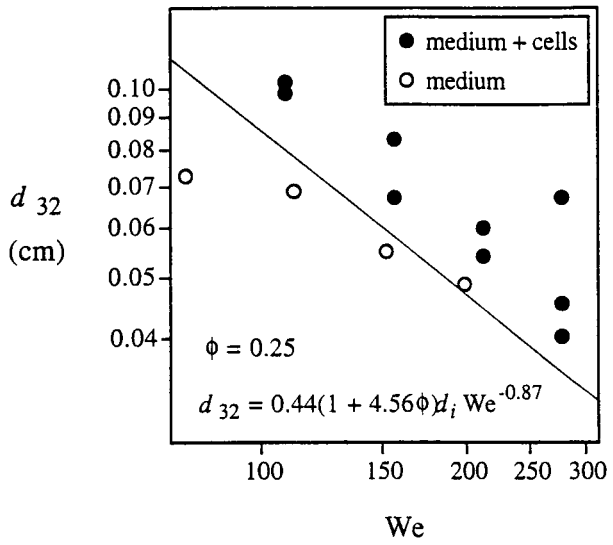

Fig. 6. Effect of cells and nutrient medium on drop size.

larger than the cells. This comparison suggests insignificant interaction between the cells and the flow.

Electrospray Contactor

The diameter of the drops produced in the stirred tank at the highest agitation speed is approx 300 μm. This size is still significantly large compared to the size of the cells. Considerably smaller droplets are produced by the electrospray nozzle of Fig. 3.

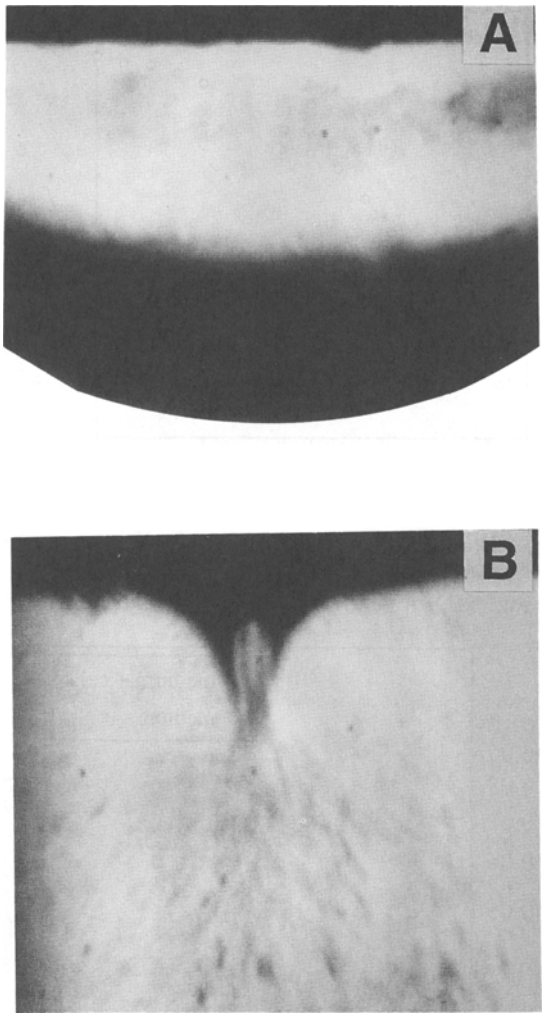

Fig. 7. Drops formed at the tip of the electrospray nozzle: **(A)** without electric field; **(B)** with electric field.

Drop Size

Pictures of drops at the tip of the metal capillary tube are presented in Fig. 7A (without electric field) and 7B (with electric field). Drop size distribution measurements shown in Fig. 8 indicate that electrospray produces significantly smaller drop sizes than agitation in stirred tanks.

Cell Growth

The effect of electrospray on cell growth was investigated by an experiment conducted over a period of 45 h using the arrangement of Fig. 3. A sample was taken from the recycle vessel of the aqueous phase every 2 h during this period to count moving cells. Results represented in Fig. 9 show that viability of SRB was maintained over a period of 45 h under electrostatic spraying.

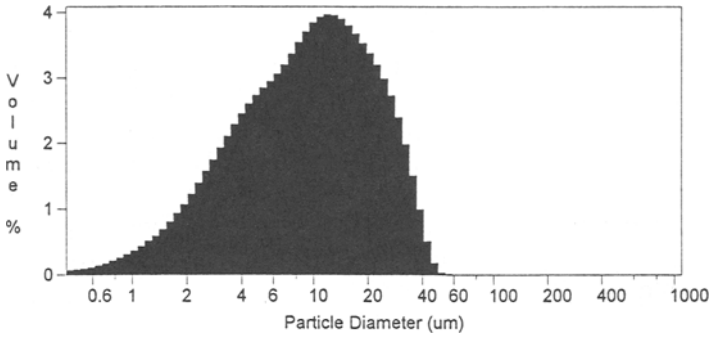

Fig. 8. Drop size distribution from the electrospray nozzle.

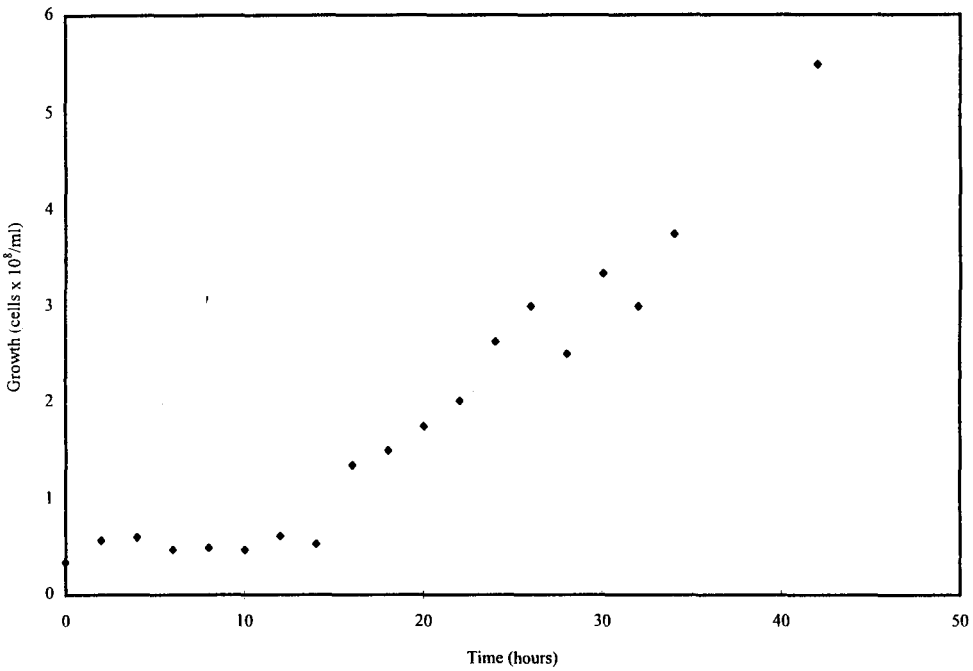

Fig. 9. Growth of SRB under electric field conditions.

SUMMARY

The hydrodynamics of a stirred-tank liquid–liquid bioreactor gave predicted average drop size as discussed in the literature. The addition of cells (SRB) in the continuous phase (aqueous) was found to increase the drop size of kerosene. A laboratory-scale electrospray bioreactor with an electrospray nozzle produced a drop size approx one order of magnitude smaller than the drop size produced by agitation in the stirred tank. Viability and growth of bacteria were maintained over a period of 45 h under electrostatic spraying. Further studies are needed to quantify the effect of the electric field on bacteria growth.

ACKNOWLEDGMENTS

Droplet size distributions were measured in the laser light scattering facility that is supported by Materials Sciences Division, Office of Basic Energy Sciences, Department of Energy. This research is supported by the Office of Oil and Gas Processing of Fossil Energy and the Fossil Energy Advanced Research and Technology Program, US Department of Energy under contract DE-AC05-84OR21400 with Martin Marietta Energy Systems Inc. The help of Mary Kathy Lee from Exxon Research and Engineering Company in conducting some of the experiments is greatly appreciated.

REFERENCES

1. Pacek, A. W., Moore, I. P. T., Nienow, A. W., and Calabrese, R. V. (1994), *AIChE J.* **40,** 1940–1949.
2. Placek, J. and Tavlarides, L. L. (1985), *AIChE J.* **31,** 1113–1120.
3. Coulaloglou, C. A. and Tavlarides, L. L. (1976), *AIChE J.* **22,** 289–297.
4. Bailey, A. G. (1984), *Phys. Bull.* **35,** 146–148.
5. Harris, M. T., Scott, T. C., and Byers, C. H. (1993), *Materials Sci. Eng.* **A168**, 125–129.
6. Scott, T. C. and Wham, R. M. (1989), *Ind. Eng. Chem. Res.* **28**, 94–97.
7. Scott, T. C., Cosgrove, J. M., DePaoli, D. W., and Sisson, W. G. (1995), *Appl. Biochem. Biotechnol.* **51/52,** 283–289.
8. Calabrese, R. V., Chang, T. P. K., and Dang, P. T. (1986), *AIChE J.* **32,** 657–666.
9. Calderbank, P. H. (1958), *Trans. Inst. Chem. Eng.* **36**, 443–459.
10. Tsouris, C. and Tavlarides, L. L. (1994), *AIChE J.* **40,** 395–406.